

# Resonant two-photon ionization spectroscopy of jet-cooled PtSi

Lian Shao, Shane M. Sickafoose, Jon D. Langenberg, Dale J. Brugh, and Michael D. Morse<sup>a)</sup>

*Department of Chemistry, University of Utah, Salt Lake City, Utah 84112*

(Received 28 October 1999; accepted 23 November 1999)

Jet-cooled diatomic PtSi, produced in a laser ablation supersonic expansion source, has been spectroscopically investigated between 17 400 and 24 000  $\text{cm}^{-1}$  by resonant two-photon ionization spectroscopy. Two vibrational progressions are observed and identified as the  $[15.7]\Omega'=1 \leftarrow X^1\Sigma^+$  and  $[18.5]\Omega'=1 \leftarrow X^1\Sigma^+$  band systems. Three bands in the former system and six bands in the latter system were rotationally resolved and analyzed, leading to bond lengths of  $r_e' = 2.1905(13)$  Å and  $r_e' = 2.2354(3)$  Å for the  $[15.7]\Omega'=1$  and  $[18.5]\Omega'=1$  states, respectively. The  $\Omega''=0$  ground state of PtSi is assigned as a  $^1\Sigma^+$  state, in agreement with previous work and with the assigned ground states of the isovalent NiC, PdC, PtC, and NiSi molecules. The ground state bond length of PtSi is given by  $r_0'' = 2.0629(2)$  Å. A Rydberg–Klein–Rees analysis of the ground and excited state potential energy curves is presented, along with a discussion of the chemical bonding and a comparison to the isoelectronic molecule, AlAu. Evidence is presented for a double bond in PtSi, as opposed to a single bond in AlAu. © 2000 American Institute of Physics. [S0021-9606(00)00707-8]

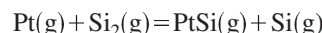
## I. INTRODUCTION

Transition metal silicides have a wide range of actual and potential applications in materials science because of their relatively high melting points, moderate densities, hardness, and resistance to chemical attack. They are used in silicon devices as barrier layer components, as Schottky-barrier rectifying contacts, low resistivity interconnecting material, and multiple quantum well devices.<sup>1</sup> The PtSi Schottky infrared detector is one of the most promising IR detectors for large focal plane array applications because of its lattice compatibility with silicon, uniformity of response, reliability, low cost, and high sensitivity.<sup>2</sup>

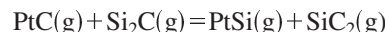
Despite their importance in materials chemistry, however, the fundamental nature of the transition metal–silicon bond has remained almost totally unexplored, at least as far as gas-phase spectroscopy is concerned. To our knowledge the only transition metal silicides to have received published spectroscopic scrutiny in the gas phase are CuSi,<sup>3</sup> AgSi,<sup>4</sup> AuSi,<sup>5–7</sup> and PtSi.<sup>8</sup> For all of these molecules cavity ring-down laser absorption spectra (CRLAS) have been recorded and rotationally analyzed by Scherer and co-workers.<sup>3,4,7,8</sup> For PtSi, nine vibronic bands in the 350 nm region were observed and assigned to a single  $^1\Sigma^+ - ^1\Sigma^+$  electronic band system through this technique, giving a ground state vibrational frequency of  $\omega_e'' = 549.0 \text{ cm}^{-1}$  and a bond length of  $r_0'' = 2.069$  Å.<sup>8</sup> In addition to this gas-phase work, the metal silicides VSi and NbSi have been investigated by matrix-isolation ESR spectroscopy and are found to have  $^2\Delta_r$  ground states in which the orbital angular momentum is partially quenched through interactions with the rare gas matrix.<sup>9</sup> Many of the bond energies of the transition metal

silicides have also been measured using Knudsen effusion mass spectrometry.<sup>10–13</sup>

Apart from the work published by the Saykally group, the only other experimental work available on molecular PtSi is a Knudsen effusion mass spectrometric determination of the dissociation energy.<sup>11</sup> Values of the third-law dissociation energies derived from the reactions



and



give the bond energy as  $D_0(\text{PtSi}) = 5.15 \pm 0.19$  eV.<sup>11</sup> To our knowledge, there are no published *ab initio* predictions of the properties of PtSi.

In this paper, we present the results of a study of jet-cooled PtSi in the visible region using resonant two-photon ionization (R2PI) spectroscopy with mass spectrometric detection. The earlier work of Paul *et al.*<sup>8</sup> is confirmed regarding the  $^1\Sigma^+$  ground state, the measurement of the ground state bond length is refined, and two new  $\Omega'=1$  excited states are examined in detail.

## II. EXPERIMENT

The resonant two-photon ionization spectrometer employed in this study has been described previously in detail<sup>14</sup> and has been extensively used for studies reported in other publications from this laboratory. The PtSi molecules were produced by the laser ablation of a Pt disk into a pulsed flow of helium containing 1% SiH<sub>4</sub>. Second-harmonic radiation of a pulsed Nd:YAG laser (532 nm, 9–12 mJ/pulse) was used to generate the Pt metal plasma, which was entrained in the He/SiH<sub>4</sub> carrier gas and swept through a channel about 2 mm in diameter and 3 cm in length prior to supersonic ex-

<sup>a)</sup>Electronic mail: Michael.Morse@chemistry.utah.edu

pansion into vacuum. To prevent the Pt disk from being drilled through by the vaporization laser and to reduce shot-to-shot fluctuations in the PtSi signal, the Pt disk was rotated and translated by a rotating disk source similar to one that has been previously described.<sup>15</sup> Although the PtSi signal was never very large, an adequate number of PtSi molecules was generated by using a moderate vaporization laser fluence and, more important, by reducing the backing pressure of the carrier gas to 30 psi (gauge).

The carrier gas of 1% SiH<sub>4</sub> in helium was prepared by carefully mixing electronic grade SiH<sub>4</sub> and research grade helium in the laboratory. To prevent accidental fires or explosions due to the pyrophoric nature of SiH<sub>4</sub>, all gases exhausted from the preparation manifold were deactivated by bubbling them through a concentrated aqueous NaOH solution prior to their release into the atmosphere.

Following expansion into vacuum, the supersonically cooled metal cluster beam was roughly collimated by passage through a 0.5-cm-diam skimmer, and admitted to the ionization region of a reflectron time-of-flight mass spectrometer. There the PtSi molecules were first excited using a tunable Nd:YAG-pumped dye laser and subsequently ionized by a pulsed excimer laser operating on ArF (193 nm, 6.42 eV). The molecular ions were then extracted at right angles to the molecular beam using a Wiley–McLaren extraction assembly.<sup>16</sup> The molecular ions traveled up a flight tube, entered a reflectron assembly, and were directed down a second flight tube to a microchannel plate detector. The resulting ion signal was preamplified, digitized, and processed by a 386 PC clone, which also controlled all of the time delays needed to successfully run the experiments.

The optical spectra of PtSi were collected by scanning the dye laser frequency while monitoring the ion signal at masses 222, 223, 224 and 226 amu, which correspond to <sup>194</sup>Pt<sup>28</sup>Si, <sup>195</sup>Pt<sup>28</sup>Si, <sup>196</sup>Pt<sup>28</sup>Si, and <sup>198</sup>Pt<sup>28</sup>Si (with natural abundances of 30.3%, 31.2%, 23.3%, and 6.6%, respectively). High resolution (0.04 cm<sup>-1</sup>) spectra were recorded by insertion of an intracavity étalon into the dye laser cavity and pressure scanning from 0 to 1 atm using Freon 12 (CCl<sub>2</sub>F<sub>2</sub>, DuPont). By simultaneously recording the I<sub>2</sub> fluorescence or absorption spectrum (or Te<sub>2</sub> absorption spectrum for regions above 20 000 cm<sup>-1</sup>) and then comparing to the I<sub>2</sub> atlas of Gerstenkorn and Luc<sup>17,18</sup> (or to the Te<sub>2</sub> atlas of Cariou and Luc<sup>19</sup>), followed by a correction for the Doppler shift due to the motion of the molecules toward the excitation radiation source, absolute line positions of all of the rotationally resolved bands were obtained. For unblended lines these are thought to be accurate to 0.01 cm<sup>-1</sup> or better.

Excited state lifetimes were measured by recording the ion signal as a function of the delay between the excitation and ionization lasers and fitting the resulting decay curves to an exponential function using a nonlinear least-squares algorithm.<sup>20</sup> Upper state lifetimes are reported as the 1/e decay time,  $\tau$ .

Due to the reactivity of SiH<sub>4</sub> with the hot filament, the ion gauge for the molecular source chamber was turned off after the pressure was stabilized at about  $2 \times 10^{-4}$  Torr. Without this precaution the filaments were found to burn out after only 1–2 days of use.

### III. RESULTS

Over the range from 17 400 to 24 000 cm<sup>-1</sup> two electronic band systems were observed and identified as  $\Omega' = 1 \leftarrow \Omega'' = 0$  systems.

#### A. The [18.5] $\Omega' = 1 \leftarrow X^1\Sigma^+$ band system

Bands are observed for this system from 19 200 to 23 700 cm<sup>-1</sup> and are listed in Table I. These bands are characterized by a head early in the *R* branch and by long upper state lifetimes (10–20  $\mu$ s). Six of the bands were examined in high resolution (0.04 cm<sup>-1</sup>), allowing precise band origins and isotope shifts to be measured. This was the key to establishing the vibrational numbering of the system.

Figure 1 displays the measured isotope shifts, defined as  $\nu_0(^{194}\text{Pt}^{28}\text{Si}) - \nu_0(^{196}\text{Pt}^{28}\text{Si})$ , as a function of band frequency,  $\nu_0(^{194}\text{Pt}^{28}\text{Si})$ . Also plotted in Fig. 1 are the theoretically predicted isotope shifts for the  $v' = 0$  bands, for three different vibrational numberings, as given by the standard expression<sup>21</sup>

$$\begin{aligned} \nu_i - \nu_j = & (\omega'_i - \omega''_i)(1 - \rho_{ij})/2 + \omega'_i(1 - \rho_{ij})v' \\ & - \omega'_i x'_i(1 - \rho_{ij}^2)(v'^2 + v') \\ & + (\omega''_i x''_i - \omega'_i x'_i)(1 - \rho_{ij}^2)/4, \end{aligned} \quad (3.1)$$

where  $\rho_{ij} = \sqrt{\mu_i/\mu_j}$ ,  $\mu_i$  is the reduced mass of the *i*th isotopic combination, and the values of  $\omega''_e$  (549.0 cm<sup>-1</sup>) and  $\omega''_e x''_e$  (1.9 cm<sup>-1</sup>) are taken from the work of Paul *et al.*<sup>8</sup> The curve giving the best agreement between measured and predicted isotope shifts assigns the lowest energy band that was rotationally resolved as the 3–0 band. The poor agreement of the other two assignments, which change the numbering by  $\pm 1$ , validates the proposed assignment.

The vibronic bands that were rotationally resolved and analyzed were fit to extract the vibrational constants of the upper state according to the standard expression<sup>21</sup>

$$\nu_{v'-0} = T_0 + \omega'_e v' - \omega'_e x'_e (v'^2 + v'), \quad (3.2)$$

resulting in the excited state spectroscopic constants  $T_0 = 18\,456.472(45)$  cm<sup>-1</sup>,  $\omega'_e = 394.873(27)$  cm<sup>-1</sup>,  $\omega'_e x'_e = 1.8120(38)$  cm<sup>-1</sup>, and  $\omega'_e y'_e = 0.007\,52(17)$  cm<sup>-1</sup> for <sup>194</sup>Pt<sup>28</sup>Si. The vibrational constants for three other isotopic modifications are also reported in Table II. Here and throughout this paper 1 $\sigma$  error limits are given in parentheses, in units of the last reported digits.

A rotationally resolved scan of the 6–0 band of <sup>194</sup>Pt<sup>28</sup>Si is displayed in Fig. 2. This is typical of the appearance of bands in this system. The spectrum is red degraded and forms a sharp bandhead toward the blue, indicating that the moment of inertia of the PtSi molecule increases upon electronic excitation. Although the PtSi molecules were rotationally somewhat warm, prohibiting observation of the first lines in the branches for some of the bands, the expected  $X^1\Sigma^+$  ground state,<sup>8</sup> the observation of all three *P*, *Q*, and *R* branches, and simulation of the branch intensities led to the assignment of the band system as the [18.5] $\Omega' = 1 \leftarrow X^1\Sigma^+$  system. Here the number in brackets designates the energy of the  $v' = 0$  level, in thousands of wave numbers. Six bands were successfully rotationally resolved and ana-

TABLE I. Vibronic band systems of  $^{194}\text{Pt}^{28}\text{Si}$ .<sup>a</sup>

System	Band	Band origin (cm <sup>-1</sup> )	$\nu_0(\text{obs}) - \nu_0(\text{calc})$ (cm <sup>-1</sup> )	Isotope shift <sup>c</sup> (cm <sup>-1</sup> )	$B'_v$ (cm <sup>-1</sup> )	$B'_v(\text{obs}) - B'_v(\text{calc})$ (cm <sup>-1</sup> )	Lifetime <sup>d</sup> ( $\mu\text{s}$ )
[18.5]1 $\leftarrow$ X0 <sup>+</sup>	2-0	19 238.70 <sup>b</sup>					
	3-0	19 619.670(2) <sup>f</sup>	0.001	0.704(2)	0.135 458(29)	-0.000 006	17.46(15)
	4-0	20 000.407(2) <sup>f</sup>	-0.002	0.941(3)	0.134 714(28)	-0.000 031	16.28(33)
	5-0	20 378.16 <sup>b</sup>					14.23(48)
	6-0	20 751.671(2) <sup>f</sup>	0.000	1.394(3)	0.133 340(24)	0.000 032	16.00(7)
	7-0	21 125.45 <sup>b</sup>					14.99(10)
	8-0	21 489.614(2) <sup>f</sup>	0.004	1.850(4)	0.131 900(25)	0.000 030	11.12(75)
	9-0	21 855.36 <sup>b</sup>					11.19(9)
	10-0 <sup>c</sup>	22 214.583(2) <sup>f</sup>	-0.005	2.280(2)	0.130 454(28)	0.000 021	10.80(50)
	11-0	22 572.330(2) <sup>f</sup>	0.002	2.484(3)	0.129 669(28)	-0.000 045	9.91(14)
	12-0	22 930.31 <sup>b</sup>					
	13-0	23 284.00 <sup>b</sup>					
	14-0	23 629.66 <sup>b</sup>					
	[15.7]1 $\leftarrow$ X0 <sup>+</sup>	5-0	17 682.260(1) <sup>f</sup>	0.000	1.148(2)	0.139 144(27)	0.000 005
6-0		18 077.476(2) <sup>f</sup>	0.000	1.435(3)	0.138 290(30)	-0.000 010	2.23(2)
7-0		18 471.914(1) <sup>f</sup>	0.000	1.707(2)	0.137 466(31)	0.000 005	2.46(8)
9-0		19 256.15 <sup>b</sup>					
10-0		19 641.85 <sup>b</sup>					

<sup>a</sup>Fitted  $B''_0$  for  $^{194}\text{Pt}^{28}\text{Si}$  is  $B''_0 = 0.162\,008(26)\text{ cm}^{-1}$ .

<sup>b</sup>Measured in low resolution, with a probable error of  $\pm 1\text{ cm}^{-1}$ ; not included in the fit of Eq. (3.2).

<sup>c</sup>Measured in high resolution as  $\nu_0(^{194}\text{Pt}^{28}\text{Si}) - \nu_0(^{196}\text{Pt}^{28}\text{Si})$ .

<sup>d</sup>Errors reported for lifetimes correspond to  $1\sigma$  in the nonlinear least-squares fit, which is probably an underestimate. A more realistic error estimate is  $\pm 10\%$  of the reported value.

<sup>e</sup> $\Lambda$ -type doubling was included for the upper state in the fit of 10-0 band only, using  $\nu = \nu_0 + B'_v J'(J'+1) \mp q'_{10} J'(J'+1)/2 - B''_v J''(J''+1)$ , where the upper sign corresponds to  $e$  levels and the lower to  $f$  levels, giving a fitted value of  $q'_{10} = -6.2(7) \times 10^{-5}$  for  $^{194}\text{Pt}^{28}\text{Si}$ . This is the accepted convention for the  $\Lambda$  doubling of  $^3\Pi_1$  states (Ref. 41). If this state is subsequently shown to be primarily of  $^1\Pi$  character, the sign of  $q'_{10}$  should be reversed to conform to accepted conventions (Ref. 41).

<sup>f</sup>Measured in high resolution, with calibration based on either the  $\text{I}_2$  atlas or  $\text{Te}_2$  atlas. Following each fitted band origin,  $B'_v$  value, and isotope shift, the  $1\sigma$  uncertainty in the fitted value is given in parentheses.

lyzed. A simultaneous fit of the measured rotational line positions of all six bands of this system and of three bands of the [15.7] $\Omega' = 1 \leftarrow X^1\Sigma^+$  system (see the following) to the formula<sup>21</sup>

$$\nu = \nu_{v'-0} + B'_v J'(J'+1) - B''_v J''(J''+1), \quad (3.3)$$

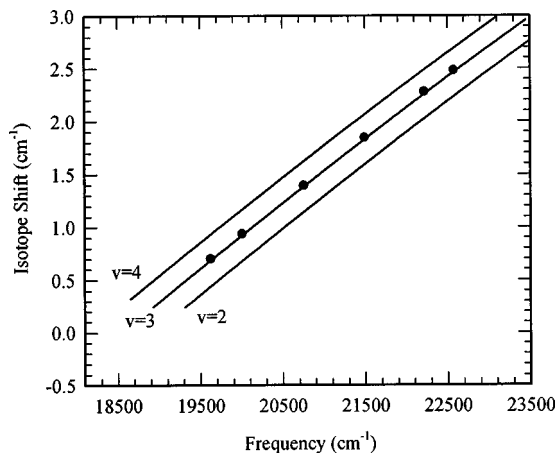


FIG. 1. Determination of the vibrational numbering of the [18.5] $\Omega' = 1 \leftarrow X^1\Sigma^+$  band system. The isotope shift, defined as  $\nu_0(^{194}\text{Pt}^{28}\text{Si}) - \nu_0(^{196}\text{Pt}^{28}\text{Si})$ , is plotted vs the band frequency for three sequential vibrational numberings, as labeled. There is best agreement between the measured and predicted isotope shifts when assigning the 19 619  $\text{cm}^{-1}$  band of  $^{194}\text{Pt}^{28}\text{Si}$  as the 3-0 band.

provided band origins  $\nu_{v'-0}$  rotational constants  $B'_v$ , for the upper levels, and a single  $B''_0$  value for the ground state, as listed in Table I. The fitted value of  $B''_0 = 0.162\,008(26)\text{ cm}^{-1}$  for  $^{194}\text{Pt}^{28}\text{Si}$  is slightly larger than the value  $0.160\,88(13)\text{ cm}^{-1}$  previously reported.<sup>8</sup> The fitted band origins for these bands were used for the isotope shift determination of the above described absolute vibrational numbering. Observed and fitted line positions for all of the rotationally resolved bands of  $^{194}\text{Pt}^{28}\text{Si}$ ,  $^{195}\text{Pt}^{28}\text{Si}$ ,  $^{196}\text{Pt}^{28}\text{Si}$ , and  $^{198}\text{Pt}^{28}\text{Si}$  are available through the Physics Auxiliary Publication Service (PAPS) of the American Institute of Physics<sup>22</sup> or from the author (M.D.M.).

The values of  $B'_v$ , for  $^{194}\text{Pt}^{28}\text{Si}$ ,  $^{195}\text{Pt}^{28}\text{Si}$ ,  $^{196}\text{Pt}^{28}\text{Si}$ , and  $^{198}\text{Pt}^{28}\text{Si}$  were fitted to the following expression,<sup>21</sup>

$$B'_v = B'_e - \alpha'_e(v + 1/2), \quad (3.4)$$

leading to the rotation-vibration constants listed in Table II. Somewhat surprisingly, the [18.5] $\Omega' = 1$  state of PtSi appears to be completely unperturbed over the range of vibrational levels examined in this report. The lack of perturbations in this system results in an excellent fit of the six measured vibronic levels to Eq. (3.2), superb agreement between isotopes of the predicted energy of the 0-0 band, which is based on an extrapolation of nearly  $800\text{ cm}^{-1}$  from the observed 2-0 band (see Table II), and an excellent fit of the measured  $B'_v$  values to Eq. (3.4). Because of the lack of perturbations in this [18.5] $\Omega' = 1$  state, the values of the

TABLE II. Fitted spectroscopic constants of PtSi.<sup>a</sup>

Electronic state	Constant	<sup>194</sup> Pt <sup>28</sup> Si	<sup>195</sup> Pt <sup>28</sup> Si	<sup>196</sup> Pt <sup>28</sup> Si	<sup>198</sup> Pt <sup>28</sup> Si
[18.5]Ω'=1	$T_0$	18 456.472(45)	18 456.566(28)	18 456.444(65)	18 456.538(56)
	$\omega'_e$	394.873(27)	394.694(18)	394.656(39)	394.365(35)
	$\omega'_e x'_e$	1.8120(38)	1.8027(27)	1.8149(55)	1.8062(54)
	$\omega'_e y'_e$	0.007 52(17)	0.007 11(13)	0.007 73(25)	0.007 40(25)
	$B'_e$	0.137 980(43)	0.137 864(25)	0.137 830(45)	0.137 627(51)
	$\alpha'_e$	0.000 719(15)	0.000 713(9)	0.000 720(15)	0.000 711(19)
	$r'_e(\text{Å})$	2.235 37(35)	2.235 58(21)	2.235 14(36)	2.235 38(42)
[15.7]Ω'=1 <sup>b</sup>	$T_0$	15 694.504	15 694.580	15 694.993	
	$\omega'_e$	399.89	399.76	399.52	
	$\omega'_e x'_e$	0.389	0.390	0.382	
	$B'_e$	0.143 753(61)	0.143 602(164)	0.143 459(79)	
	$\alpha'_e$	0.000 839(24)	0.000 827(64)	0.000 817(31)	
	$r'_e(\text{Å})$	2.190 02(46)	2.190 46(125)	2.190 85(60)	
$X\Omega''=0^+$	$B''_0$	0.162 008(26)	0.161 911(27)	0.161 814(32)	0.161 617(38)
	$r''_0(\text{Å})$	2.062 95(17)	2.062 90(17)	2.062 85(20)	2.062 81(24)

<sup>a</sup>All spectroscopic constants are reported in cm<sup>-1</sup> unless specified. Values given in parentheses represent the 1σ error limit of the fitted parameter, in units of the last digit quoted.

<sup>b</sup>Reported  $T_0$ ,  $\omega'_e$ ,  $\omega'_e x'_e$  were extracted by fitting the rotationally resolved bands 5-0, 6-0, 7-0 to the formula  $\nu_{v',-0} = T_0 + \omega'_e v' - \omega'_e x'_e (v'^2 + v')$ . Because three parameters were extracted from three pieces of data, no error estimate was possible for these vibrational parameters.

<sup>194</sup>Pt<sup>28</sup>Si, <sup>195</sup>Pt<sup>28</sup>Si, and <sup>196</sup>Pt<sup>28</sup>Si constants were used to perform a Rydberg–Klein–Rees (RKR) calculation of the potential using the RKR1 program of LeRoy,<sup>23</sup> as described in Sec. III C.

### B. The [15.7]Ω'=1 ← X<sup>1</sup>Σ<sup>+</sup> band system

To the red of the [18.5]Ω'=1 ← X<sup>1</sup>Σ<sup>+</sup> system lies a second band system which ranges from 17 400 to 19 200 cm<sup>-1</sup>, and is also characterized by Ω'=1. The observed vibronic band positions for this system are reported in Table I. Three out of five observed bands in this system were rotationally resolved and analyzed for <sup>194</sup>Pt<sup>28</sup>Si, <sup>195</sup>Pt<sup>28</sup>Si, and <sup>196</sup>Pt<sup>28</sup>Si. The bands are quite similar in appearance to the band system described above with *R*, *Q*, and *P* branches and a bandhead early in the *R* branch. The facts that these bands

have rather shorter lifetimes (~2 μs) and larger upper state rotational constants (see Table I) demonstrate that the excited state is of a different origin than the [18.5]Ω'=1 state.

The vibrational numbering of the bands corresponding to the assignment given in Table I was established in the same way as described for the [18.5]Ω'=1 ← X<sup>1</sup>Σ<sup>+</sup> band system. Although only three data points are available, Fig. 3 demonstrates that the lowest wave number band that was rotationally resolved corresponds to  $v'=5$ . At the time these data were recorded we were unable to continue our rotationally resolved studies on any of the remaining bands, and are therefore unable to report error limits for the vibrational constants  $T_0$ ,  $\omega'_e$ , and  $\omega'_e x'_e$  listed in Table II. These were ob-

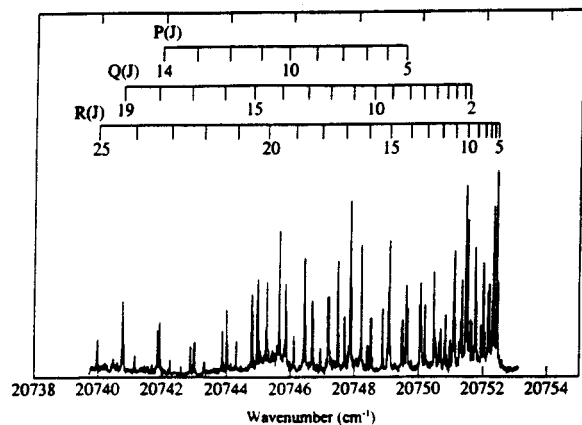


FIG. 2. Rotationally resolved scan over the 6-0 band of <sup>194</sup>Pt<sup>28</sup>Si with the three observed branches labeled. The positions of the low-*J* lines *R*(0), *R*(1), *R*(2), *R*(3), *R*(4), *Q*(1), *P*(2), *P*(3), and *P*(4) are not indicated because of the small amount of space available. All except for *P*(2), *Q*(1), and *R*(3) could be identified in the spectrum, however.

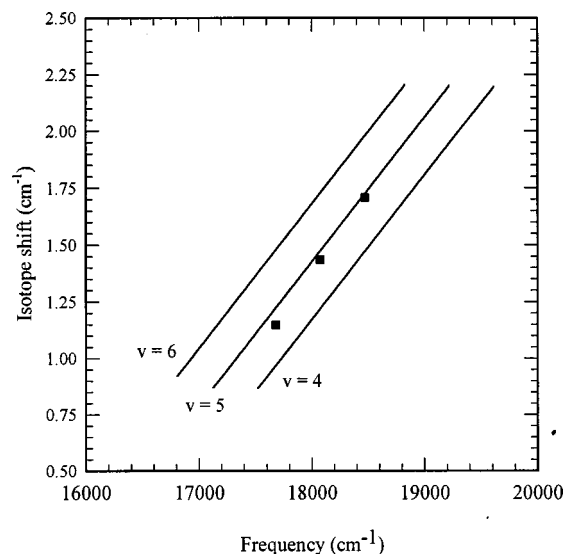


FIG. 3. Determination of the vibrational numbering of the [15.7]Ω'=1 ← X<sup>1</sup>Σ<sup>+</sup> band system. The best agreement between the measured and predicted isotope shifts is achieved when assigning the 17 682 cm<sup>-1</sup> band of <sup>194</sup>Pt<sup>28</sup>Si as the 5-0 band.

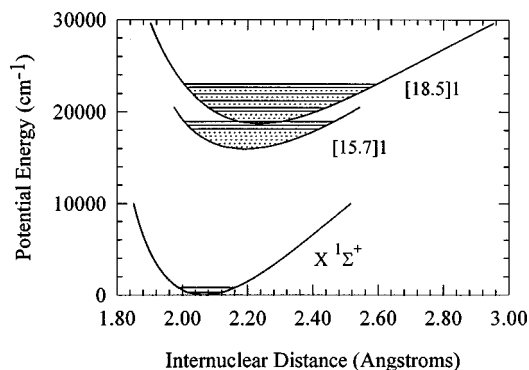


FIG. 4. Potential energy curves for the PtSi molecule. The ground state RKR curve is based on the values of  $\omega_e''$ ,  $\omega_e''x_e''$ , and  $\alpha_e''$  reported by Paul *et al.* (Ref. 8) along with our improved value of  $B_0''$ .

tained by fitting the band origins of the three rotationally resolved bands to formula (3.2). Since the number of fitted parameters matched the number of data points, no error estimate was possible. The values of the rotation–vibration constants  $B_e'$ ,  $\alpha_e'$ , and  $r_e'$  for  $^{194}\text{Pt}^{28}\text{Si}$ ,  $^{195}\text{Pt}^{28}\text{Si}$ , and  $^{196}\text{Pt}^{28}\text{Si}$  are also summarized in Table II for this band system.

### C. RKR analysis of the $X^1\Sigma^+$ , [15.7]1, and [18.5]1 states

Because of the excellent quality of the data for the [18.5]1 state, it was decided to perform a Rydberg–Klein–Rees (RKR) analysis of the potential energy curves for PtSi, in the hope that these will be useful for comparisons to *ab initio* calculations on this system. The calculations were performed using the RKR1 program, written and freely distributed by LeRoy.<sup>23</sup> The RKR calculations for the [15.7]1 and [18.5]1 states were performed separately on the  $^{194}\text{Pt}^{28}\text{Si}$ ,  $^{195}\text{Pt}^{28}\text{Si}$ , and  $^{196}\text{Pt}^{28}\text{Si}$  isotopic modifications, with excellent agreement between the isotopes. The resulting potential energy curves are displayed in Fig. 4, which also displays the vibrational levels that were rotationally resolved as solid lines. Although curves obtained from the separate analyses of the  $^{194}\text{Pt}^{28}\text{Si}$ ,  $^{195}\text{Pt}^{28}\text{Si}$ , and  $^{196}\text{Pt}^{28}\text{Si}$  isotopic modifications are displayed in Fig. 4, they cannot be discerned because they are coincident on the scale of this figure. Rotationally unresolved levels lying below the resolved levels are displayed as dotted lines. The potential energy curve of the  $X^1\Sigma^+$  ground state is a RKR curve based on the vibrational ( $\omega_e'' = 549.0\text{ cm}^{-1}$ ,  $\omega_e''x_e'' = 1.9\text{ cm}^{-1}$ ) and rotational ( $\alpha_e'' = 0.00102\text{ cm}^{-1}$ ) constants provided by Paul *et al.*,<sup>8</sup> supplemented by our more accurate determination of  $B_0''$ . Values of the RKR turning points for the  $X^1\Sigma^+$ , [15.7]1, and [18.5]1 states are available through the Physics Auxiliary Publication Service (PAPS) of the American Institute of Physics<sup>22</sup> or from the author (M.D.M.).

## IV. DISCUSSION

In this work and the work of Paul *et al.*,<sup>8</sup> the bond length of PtSi [ $r_0'' = 2.0629(2)\text{ \AA}$ ] is determined to be significantly shorter than that of the isoelectronic molecule AlAu [ $r_e''$

$= 2.3382\text{ \AA}$ ].<sup>24</sup> Likewise, the bond energy estimated for PtSi from Knudsen effusion mass spectrometry [ $D_0(\text{PtSi}) = 5.15 \pm 0.19\text{ eV}$ ]<sup>11</sup> is much greater than that estimated for AlAu [ $D_0(\text{AlAu}) = 3.34 \pm 0.07\text{ eV}$ ] using the same method.<sup>25</sup> In agreement with this trend, the ground state vibrational frequency of PtSi ( $549.0\text{ cm}^{-1}$ )<sup>8</sup> is also much larger than that of AlAu ( $333.00\text{ cm}^{-1}$ ).<sup>24</sup> These results suggest that the chemical bonding in the two molecules is really quite different, despite the fact that they are isoelectronic.

The electronic structure of the coinage metal aluminides AlCu<sup>26</sup>, AlAg<sup>27</sup> and AlAu<sup>24</sup> is quite straightforward for the ground electronic state. In a molecular orbital description, the  $3p\sigma$  orbital of aluminum combines with the  $ns$  orbital of the coinage metal atom to form a  $\sigma$  bonding orbital which is doubly occupied, giving a nominal bond order of 1. An alternative possibility is that the ground state derives from the  $\text{Al}^+$ ,  $^1\text{S}+\text{M}^-$ ,  $^1\text{S}$  separated ion limit, implying substantial  $\text{Al}^+\text{M}^-$  character in the AlCu, AlAg and AlAu molecules. Both descriptions result in  $^1\Sigma^+$  ground states for the coinage metal aluminides, and there is, of course, substantial mixing between these covalent and ionic descriptions. The true character of the molecule lies between these pure descriptions of the bond. In either case, however, the coinage metal aluminides are characterized by a single  $\sigma$  bond. The possibility of  $\pi$  bonding is severely disfavored, since the only way in which a  $\pi$  bond can be formed is by  $d\pi$  electron pair donation from the more electronegative coinage metal atom to the empty  $3p\pi$  orbital of the electropositive aluminum atom. Although some delocalization of the coinage metal  $d\pi$  electrons in this way undoubtedly occurs, the process cannot be very significant because the direction of electron transfer runs counter to the atomic electronegativities.

The ground electronic state of the isoelectronic PtSi molecule is an  $\Omega=0$  state, and this is almost certainly also a  $^1\Sigma^+$  state. The isovalent molecules NiC,<sup>28–30</sup> PdC,<sup>31,32</sup> PtC,<sup>33–37</sup> and NiSi<sup>28,38–40</sup> are all known to possess a  $^1\Sigma^+$  ground state, and there is no reason to expect anything different for PtSi. In this molecule the ground state may be considered to derive from the  $\text{Pt } 5d^9 6s^1$ ,  $^3D + \text{Si } 3s^2 3p^2$ ,  $^3P$  separated atom limit. The  $\sigma$  bond then results from the combination of the Pt  $6s$  orbital with the Si  $3p\sigma$  orbital to form a bonding molecular orbital containing two electrons. The remaining  $3p$  electron of silicon must then lie in an orthogonal  $3p\pi$  orbital in order to retain the favorable  $^3P$  angular momentum coupling. If the hole in the  $5d$  shell of Pt is in a  $5d\pi$  orbital, the opportunity then exists of spin-pairing these electrons to form a  $\pi$  bond in PtSi. Unlike AlAu, where such a possibility would require both electrons in the  $\pi$  bond to come from the more electronegative Au atom, the  $\pi$  bond in PtSi would be of a more covalent nature, with one of the  $\pi$  electrons originating from Pt, and one from Si. The highly disfavored donation of two  $\pi$  electrons from the more electronegative to the more electropositive atom that is required in AlAu is turned into a more equal sharing of the charge in PtSi. The formation of this  $\pi$  bond explains the dramatically shorter bond length, greater bond strength, and higher vibrational frequency of PtSi as compared to AlAu. In short, PtSi has a double bond while AlAu has only a single bond.

## V. CONCLUSIONS

A resonant two-photon ionization study of jet-cooled PtSi has led to the identification of two new band systems, both of which have  $\Omega=1$ . Rotationally resolved spectroscopy has permitted the rovibrational spectroscopic constants for these states to be measured, and has led to an improved value of  $B_0''$  for the ground state. RKR potential curves for the ground state and both  $\Omega=1$  excited states are presented. From this work a ground state bond length of  $r_0'' = 2.0629(2)$  Å is derived. A comparison of the bond lengths, bond energies, and vibrational frequencies of the isoelectronic molecules PtSi and AlAu demonstrates the importance of  $\pi$  bonding in PtSi, and the absence of  $\pi$  bonding in AlAu. This is rationalized on the basis of the electronegativity difference between Al and Au.

## ACKNOWLEDGMENTS

We thank the National Science Foundation for support of this research under Grant No. CHE-9626557. Acknowledgment is also made to the donors of the Petroleum Research Fund, administered by the American Chemical Society, for partial support of this work. Finally, the authors wish to express their gratitude to Professor Tim Steimle for his gift of the isotopically pure  $^{130}\text{Te}$  and sealed absorption cell used to calibrate the rotationally resolved spectra collected here.

- <sup>1</sup>B. J. Aylett, *Br. Polym. J.* **18**, 359 (1986).
- <sup>2</sup>T. L. Lin, J. S. Park, S. D. Gunapala, E. W. Jones, and H. M. del Castillo, *Jpn. J. Appl. Phys., Part 1* **33**, 2435 (1994).
- <sup>3</sup>J. J. Scherer, J. B. Paul, C. P. Collier, and R. J. Saykally, *J. Chem. Phys.* **102**, 5190 (1995).
- <sup>4</sup>J. J. Scherer, J. B. Paul, C. P. Collier, and R. J. Saykally, *J. Chem. Phys.* **103**, 113 (1995).
- <sup>5</sup>R. F. Barrow, W. J. M. Gissane, and D. N. Travis, *Nature (London)* **201**, 603 (1964).
- <sup>6</sup>C. Coquant and R. Houdart, *C. R. Hebd. Seances Acad. Sci., Ser. B* **284**, 171 (1977).
- <sup>7</sup>J. J. Scherer, J. B. Paul, C. P. Collier, A. O'Keefe, and R. J. Saykally, *J. Chem. Phys.* **103**, 9187 (1995).
- <sup>8</sup>J. B. Paul, J. J. Scherer, C. P. Collier, and R. J. Saykally, *J. Chem. Phys.* **104**, 2782 (1996).
- <sup>9</sup>Y. M. Hamrick and W. Weltner, Jr., *J. Chem. Phys.* **94**, 3371 (1991).
- <sup>10</sup>A. V. Auwera-Mahieu, N. S. McIntyre, and J. Drowart, *Chem. Phys. Lett.* **4**, 198 (1969).
- <sup>11</sup>A. V. Auwera-Mahieu, R. Peeters, N. S. McIntyre, and J. Drowart, *Trans. Faraday Soc.* **66**, 809 (1970).
- <sup>12</sup>J. E. Kingcade, Jr. and K. A. Gingerich, *J. Chem. Phys.* **84**, 4574 (1986).
- <sup>13</sup>J. E. Kingcade, Jr. and K. A. Gingerich, *J. Chem. Soc., Faraday Trans. 2* **85**, 195 (1989).
- <sup>14</sup>Z. Fu, G. W. Lemire, Y. M. Hamrick, S. Taylor, J.-C. Shui, and M. D. Morse, *J. Chem. Phys.* **88**, 3524 (1988).
- <sup>15</sup>S. C. O'Brien, Y. Liu, Q. Zhang, J. R. Heath, F. K. Tittel, R. F. Curl, and R. E. Smalley, *J. Chem. Phys.* **84**, 4074 (1986).
- <sup>16</sup>W. C. Wiley and I. H. McLaren, *Rev. Sci. Instrum.* **26**, 1150 (1955).
- <sup>17</sup>S. Gerstenkorn and P. Luc, *Atlas du Spectre d'Absorption de la Molécule d'Iode entre 14,800–20,000 cm<sup>-1</sup>* (CNRS, Paris, 1978).
- <sup>18</sup>S. Gerstenkorn and P. Luc, *Rev. Phys. Appl.* **14**, 791 (1979).
- <sup>19</sup>J. Cariou and P. Luc, *Atlas du Spectre d'Absorption de la Molécule de Tellure entre 18,500–23,800 cm<sup>-1</sup>* (CNRS, Paris, 1980).
- <sup>20</sup>P. R. Bevington, *Data Reduction and Error Analysis for the Physical Sciences* (McGraw-Hill, New York, 1969).
- <sup>21</sup>G. Herzberg, *Molecular Spectra and Molecular Structure I. Spectra of Diatomic Molecules*, 2nd ed. (Van Nostrand Reinhold, New York, 1950).
- <sup>22</sup>See EPAPS Document No. E-JCPSA6-112-007007 for 25 pages of absolute line positions, fits of  $B_v$  values, vibronic fits, and RKR fits. This document may be retrieved via the EPAPS homepage (<http://www.aip.org/pubservs/epaps.html>) or from <ftp.aip.org> in the directory /epaps/. See the EPAPS homepage for more information.
- <sup>23</sup>R. J. LeRoy, *Chemical Physics Research Report No. CP-425*, University of Waterloo, Waterloo, 1992.
- <sup>24</sup>R. F. Barrow and D. N. Travis, *Proc. R. Soc. London, Ser. A* **273**, 133 (1963).
- <sup>25</sup>K. A. Gingerich and G. D. Blue, *J. Chem. Phys.* **59**, 185 (1973).
- <sup>26</sup>J. M. Behm, C. A. Arrington, J. D. Langenberg, and M. D. Morse, *J. Chem. Phys.* **99**, 6394 (1993).
- <sup>27</sup>D. L. Robbins, C. S. Yeh, J. S. Pilgrim, G. L. Lang, and M. A. Duncan, *J. Chem. Phys.* **100**, 4775 (1994).
- <sup>28</sup>I. Shim and K. A. Gingerich, *Z. Phys. D: At., Mol. Clusters* **12**, 373 (1989).
- <sup>29</sup>I. Shim and K. A. Gingerich, *Chem. Phys. Lett.* **303**, 87 (1999).
- <sup>30</sup>D. J. Brugh and M. D. Morse (unpublished).
- <sup>31</sup>N. Russo, J. Andzelm, and D. R. Salahub, *Chem. Phys.* **114**, 331 (1987).
- <sup>32</sup>J. D. Langenberg, L. Shao, and M. D. Morse, *J. Chem. Phys.* **111**, 4077 (1999).
- <sup>33</sup>R. Scullman and B. Yttermo, *Ark. Fys.* **33**, 231 (1966).
- <sup>34</sup>O. Appelblad, R. F. Barrow, and R. Scullman, *Proc. Phys. Soc. London* **91**, 260 (1967).
- <sup>35</sup>O. Appelblad, C. Nilsson, and R. Scullman, *Phys. Scr.* **7**, 65 (1973).
- <sup>36</sup>T. C. Steimle, K. Y. Jung, and B.-Z. Li, *J. Chem. Phys.* **102**, 5937 (1995).
- <sup>37</sup>T. C. Steimle, K. Y. Jung, and B.-Z. Li, *J. Chem. Phys.* **103**, 1767 (1995).
- <sup>38</sup>I. Shim and K. A. Gingerich, *Z. Phys. D: At., Mol. Clusters* **16**, 141 (1990).
- <sup>39</sup>H. Haberlandt, *Chem. Phys.* **138**, 315 (1989).
- <sup>40</sup>N. F. Lindholm, D. J. Brugh, G. K. Rothschof, S. M. Sickafoose, and M. D. Morse (unpublished).
- <sup>41</sup>J. M. Brown and A. J. Merer, *J. Mol. Spectrosc.* **74**, 488 (1979).